Fermi National Accelerator Laboratory

FERMILAB-Pub-76/102-EXP
1184.000

(Submitted to Medical Physics)

PHYSICAL CHARACTERIZATION OF NEUTRON BEAMS PRODUCED BY PROTONS AND DEUTERONS OF VARIOUS ENERGIES BOMBARDING BERYLLIUM AND LITHIUM TARGETS OF SEVERAL THICKNESSES

H. I. Amols and J. F. Dicello
University of California, Los Alamos Scientific Laboratory
Los Alamos, New Mexico 87545

and

M. Awschalom and L. Coulson
Fermi National Accelerator Laboratory, Batavia, Illinois 60510

and

S. W. Johnsen and R. B. Theus
Crocker Nuclear Laboratory, University of California
Davis, California 95616

December 1976

Operated by Universities Research Association Inc. under contract with the Energy Research and Development Administration

Fermilab-Pub. 76-102-Exp.
1184.000

PHYSICAL CHARACTERIZATION OF NEUTRON BEAMS PRODUCED BY PROTONS AND DEUTERONS OF VARIOUS ENERGIES BOMBARDING BERYLLIUM AND LITHIUM TARGETS OF SEVERAL THICKNESSES

H. I. Amols,[a] M. Awschalom,[b] L. Coulson,[b]
J. F. Dicello,[a] S. W. Johnsen[c] R. B. Theus[d]

December 1976

ABSTRACT

Protons of 35 and 65 MeV and deuterons of 35 MeV were used to bombard beryllium and lithium targets of various thicknesses.

Four types of experiments were conducted in order to characterize the neutron fields. They were:

1. central axis depth dose measurements in a water phantom,
2. dose build-up at small depths in tissue equivalent plastic,
3. microdosimetric measurements and LET-distributions,
4. neutron yields and energy spectra at zero degrees.

The results generally show that:

1. the central axis depth doses for the 35 MeV and 65 MeV particles roughly approximate those of

^{60}Co and 4 MeV bremmstrahlung photons respectively,

2. the neutron dose build-ups are more rapid than those of the above mentioned photon sources,

3. the microdosimetric spectra show differences which are consistent with the measured neutron energy spectra,

4. p-Li compared to p-Be neutron spectra have larger high energy particle flux for similar target and beam configurations.

This research was supported in part by the following foundations and government agencies: National Cancer Institute, Grants #1PO CA 18081-01 and PHS CA 17419-01, American Cancer Society, Illinois Division, Grants #75-17 and 76-10, Illinois Cancer Council, and ERDA.

(a) University of California, Los Alamos Scientific Laboratory, Los Alamos, New Mexico 87545

(b) Fermi National Accelerator Laboratory, Batavia, Illinois 60510

(c) Crocker Nuclear Laboratory, University of California, Davis, California 95616

(d) Crocker Nuclear Laboratory, on leave from the Naval Research Laboratory, Washington, D. C.

INTRODUCTION

While planning a neutron beam irradiation facility for cancer therapy research at the Fermi National Accelerator Laboratory, it was deemed necessary to characterize physically a number of potentially useful neutron beams. The available proton beam could have any energy between 37.54 and 66.18 MeV. Hence, the characteristics of the forward scattered neutron beams created during the bombardment of the lithium and beryllium targets of various thicknesses were studied as well as those of neutron beams due to 35 MeV deuterons incident on beryllium. These measurements were done in conjunction with personnel from a medical accelerator development project at LASL.[1]

Four types of measurements were considered minimal for initial characterization of the neutron beams:

1. a. central axis depth dose with ionization chambers,
   b. dose build-up from small depths to beyond the depth of maximum dose per incident fluence with extrapolation ionization chambers,
2. microdosimetry with Rossi-type spherical detector,
3. neutron energy spectra by time-of-flight.

All the measurements were taken at zero degrees. All results except those for microdosimetry were normalized per unit solid angle and per microCoulomb of charged particles incident on the

targets. The neutron beams created by deuterium were studied to allow comparisons with published data.[2]

Although the present measurements have produced a large amount of data, they were designed only as a preliminary study. Flatness of dose as a function of polar angle, variation of neutron energy spectra, gamma ray component of the total dose, and microdosimetry as a function of depth in tissue equivalent material, were not studied. Additionally, the uncertainties associated with the present data may be unacceptable for some applications.

EXPERIMENTAL SET-UP

These measurements were performed using the 76-inch isochronous cyclotron at the University of California, Davis.[3] The charged particle beams were directed successively onto eight targets mounted in a target wheel. The neutrons emanating at 0° from the incident beam were collimated by a 1.5 m long steel collimator with a rectangular opening 5.7 cm by 7.0 cm. The collimator exit was 2.85 m from the upstream face of the targets.

Charged particles exiting the traget were swept out of the neutron beam by a magnet placed between the target wheel and the collimator.

The incident beam current was measured by placing a 0.012 mm thick aluminum foil upstream of the target wheel in the charged particle beam and measuring the secondary electron emission current

produced by the particles traversing the foil. This system was calibrated by comparison of the secondary electron emission current against a Faraday cup current. This calibration was repeated periodically throughout the course of the experiment.

Targets

Natural lithium and beryllium were used as targets.

The Li targets were sealed under vacuum inside stainless steel cases. These cases had one inch inside diameters and 0.025 cm stainless steel entrance windows. They were machined from commercially available Li extrusions.

The windows caused an energy degradation of the incident beam. Hence, to equalize incident energies on the lithium and the beryllium targets, 0.025 cm stainless steel absorbers were also placed on the upstream side of the beryllium targets.

The thicknesses of the targets were chosen such that protons traversing them and having incident energies of 65 MeV would loose either all their energy, 50, 40, 30, or 20 MeV by ionization. These thicknesses were calculated using Janni's tables.[4] The thickness tolerance was such that the actual target would cause the stated energy loss plus or minus 0.5 MeV.

The various target configurations are summarized in Table I.

TABLE I

Target Lengths

Energy Loss by Ionization (MeV)	65	50	40	30	20
			Beryllium		
Thickness (cm)	2.412	2.212	1.957	1.603	1.155
± Tolerance (cm)	0.033	0.010	0.015	0.020	0.025
			Lithium		
Thichness (cm)	7.993	7.338	6.498	5.325	3.841
± Tolerance (cm)	0.110	0.033	0.051	0.067	0.082

NEUTRON ENERGY SPECTRA

Experimental Technique

Neutron yield and energy spectra were measured for 65.4 MeV protons, 35 MeV protons and 35 MeV deuterons incident upon selected targets. The actual accelerated beam energies were 65.6 MeV and 37.5 MeV for the protons and 39.2 MeV for the deuterons to allow for energy degradation in the windows.

The detector used for these measurements was a cylindrical NE213* liquid scintillator, 5.08 cm long by 5.08 cm diameter mounted coaxially in the neutron beam. The efficiency of the detector as a function of incident neutron energy had been calculated using a modified version of the Monte Carlo code by Stanton.[5]

*Nuclear Enterprises, Ltd.

In a previous experiment, the efficiency of the detector had been measured at several energies to investigate the accuracy of the calculated values.[6] Pulse shape discrimination techniques were used to distinguish events initiated by gamma rays from those attributed to neutrons.

The detector was placed 2.90 m downstream from the target wheel and was fully illuminated by the neutron beam. The neutron time-of-flight was measured relative to a stop signal from the cyclotron r.f.

The measured target-to-detector distance, and the position of the gamma ray peak relative to the rest of the time-of-flight spectra were used to calibrate the neutron flight times. The longest flight times observed were limited by the overlapping of successive beam bursts, giving a threshold of five to nine MeV.

Results

The measured neutron spectra are displayed in Figs. 1 through 3. Figures 1 and 2 show spectra obtained from 65.4 MeV protons incident upon beryllium and lithium targets, respectively. The energy resolution corresponding to 65 MeV neutron energy is ± 5 MeV. The overlapping of beam bursts and the finite time resolution of the detection system, together with phase shifts of the beam bursts relative to the cyclotron r.f., lead to some uncertainties in the shape of the spectra. For example, the curves do not pass through zero at the kinematic limit. The Q-values of the $^{9}Be(p,n)^{9}B$ and $^{7}Li(p,n)^{7}Be$ reactions are -1.85 and -1.64 MeV respectively, hence,

we would not expect neutrons above 63.8 MeV.

These plots show that the thinner targets produce harder spectra as expected. The increase in yield shown in changing from a target which stops the beam to a slightly thinner one is attributed to the absorption of neutrons by the thick target. The additional target material used to stop the beam, produces few neutrons in the energy range measurable, yet attenuates neutrons produced in the upstream portions of the target.

Figure 3 shows spectra measured for 35 MeV protons and deuterons incident upon the 1.16 cm beryllium and 3.84 cm lithium targets. The p-Li and p-Be spectra indicate a large low energy component of evaporation neutrons, as also evidenced in other work.[7] The lithium spectrum has a larger high energy component reflecting a larger neutron production cross section for the inclusive p-Li reaction than for p-Be near the kinematic limit.[8] The d-Li and d-Be spectra display the characteristic shape associated with stripping reactions. The beryllium data agree with other work[9] within the accuracy of the measurements.

The neutron yield for these spectra is tabulated in Table II. The overall uncertainty in the yield, including beam current integration and detector efficiency, is ± 25%.

Table II

Integral yield of neutrons produced by bombarding lithium and beryllium targets with protons and deuterons.

Beam Energy MeV	Particle Type	Incident Energy MeV	Target Thickness cm	Target Mat'l	Yield Neutrons/ μC/sr	Cut Off Energy MeV
65.6	prot	65.4	2.41	Be	8.8×10^{10}	9.1
"	"	"	2.21	Be	9.4×10^{10}	"
"	"	"	1.96	Be	8.8×10^{10}	"
"	"	"	1.60	Be	7.0×10^{10}	"
"	"	"	7.99	Li	10.6×10^{10}	"
"	"	"	7.34	Li	10.9×10^{10}	"
"	"	"	6.50	Li	10.7×10^{10}	"
"	"	"	5.33	Li	9.4×10^{10}	"
37.5	"	35	1.16	Be	1.6×10^{10}	5.1
"	"	"	3.84	Li	1.7×10^{10}	5.1
39.2	deut	"	1.16	Be	19.1×10^{10}	5.0
"	"	"	3.84	Li	21.3×10^{10}	5.0

CENTRAL AXIS DEPTH DOSE DISTRIBUTIONS

These depth dose measurements were made in a water phantom measuring 50 cm x 41 cm x 40 cm, along the central axis of the neutron beam. Water was chosen for the phantom fill because of ease of handling and because it has been used in two international neutron dose intercomparisons.[10] The entrance window of the phantom was an acrylic sheet 1.6 mm thick and 15 cm x 15 cm in cross section.

Measurements were made with a 0.1 cm^3 ionization chamber with tissue-equivalent walls.[11,12] This chamber was filled with air for most of the measurements. Some measurements were repeated using a tissue-equivalent gas for 35 MeV incident particles. This chamber was calibrated at LASL and EG&G, using ^{60}Co gamma sources and at LASL with 250 keVp x-rays.

A 1 cm^3 ionization chamber placed immediately downstream of the phantom was used as a secondary monitor. The primary flux monitor was the previously described aluminum foil in the charged particle beam. The charges from these three sources were integrated during each measurement. The dose was calculated using the formulation given by Attix et al.,[2] taking into account the gamma ray dose in the incident neutron beam component measured by microdosimetric technique.

The exact values for several of the constants needed for dosimetry are not yet known. Hence, their values were taken to be those in use at the M. D. Anderson Hospital[13] for the neutrons

resulting from 50 MeV deuterons incident on a thick beryllium target. The precision in doses is calculated to be better than ± 10%, and the total uncertainty is estimated to be better than ± 20%. Then,

$$\text{Dose} = 2.13 \times 10^{10} \ (g + 0.986\ n)\ Q(C)\ \text{rad}$$

where g and n are the gamma and neutron fractions of the total dose, and Q is the collected charge (Coulomb).

The values of g and n used to evaluate this equation, as well as the dose per microCoulomb, at D_{max}, at 125 cm TSD are given in Table III.

Table III

Gamma and neutron fractions of the total dose and dose/μC at 125 cm TSD.

Beam	Target Thickness cm	g	n	$D(\frac{\text{mrad}}{\mu C})$
p(65)-Be	2.41	0.02	0.98	57
	2.21	0.03	0.97	---
	1.96	0.04	0.96	---
	1.60	0.05	0.95	49
p(65)-Li	7.99	0.03	0.97	64
	7.34	0.03	0.97	---
	6.50	0.04	0.96	---
	5.33	0.04	0.96	58
p(35)-Be	1.16	0.06	0.94	16
p(35)-Li	3.84	0.07	0.93	14
d(35)-Be	1.16	0.04	0.96	104
d(35)-Li	3.84	0.03	0.97	96

Results

Figures 4 and 5, show the results in terms of rad/μC of incident 65 MeV protons on lithium and beryllium targets, respectively, as a function of depth. The Fermilab results were obtained with 66.18 MeV protons incident on a 2.21 cm thick Be-target. These figures show a slight decrease in the relative spread of dose/μC as a function of depth in the phantom which is qualitatively consistent with a monotonic decrease in dose attenuation with increasing average neutron energy. Unfortunately the uncertainties do not allow a quantitative analysis.

Figures 6 and 7 show similar results for 35 MeV protons and deuterons on thick lithium and beryllium targets.

The smaller value for the measured depth for $D_{max}/2$, with respect to Fermilab results, could be attributed to the smaller beam cross section. For this experiment, the neutron beam cross section at the phantom entrance was 6.9 cm x 8.6 cm, while at Fermilab it was 10 cm x 10 cm. No correction was made for the difference in densities of the fluids used in the phantoms. At Fermilab, Frigerio's[14] TE solution (ρ = 1.068 g/cm^3) was used in the phantom.

Dose Build Up Measurements

These measurements were made with an air-filled, tissue equivalent extrapolation chamber,[15] mounted inside a block of tissue equivalent plastic, 10 cm x 10 cm x 4.7 cm.

This chamber was used with a plate spacing of 3.25 mm, at polarizing voltages of + and - 500 volts. Two references for

the incident neutron flux normalizing factors were used, a 1 cm^3 tissue equivalent chamber mounted slightly off axis, and the in-beam aluminum foil monitor previously described.

The results are given in Figs. 8, 9, and 10 for 65 MeV and 35 MeV protons and 35 MeV deuterons. Fermilab results from 66.17 MeV on 2.21 cm Be are also given.

The differences in the measured dose rates as a function of depth for the 65 MeV protons on the Be- and Li-targets were small and possibly monotonically varying with average neutron energy. The differences between Fermilab and these results at 2.9 mg/cm^2 may be a result of differences in collimation. The collimator used in this experiment had parallel steel sides. The collimator at Fermilab was made of polyethylene loaded concrete with a truncated pyramidal opening. The results for 35 MeV deuterons on a thick Be-target are in agreement with NRL data.[2]

Error Analysis

The uncertainties in dose/μC of incident beam may be divided into two classes, a) dosimetry constants such as ionization chamber calibration, stopping powers, kerma ratios, energies for the creation of electron-ion pairs, etc; b) quantities measured in the course of this experiment such as distance, charge, temperature and pressure. The uncertainties attributed to these various quantities are discussed below.

1 - Ionization chamber calibration, ± 3%

2 - The combination of stopping powers, kerma ratios, and energies for ion-pair creation, ±10%

3 - distance ± 0.3%

4 - temperature ± 0.3%

5 - pressure ± 0.7%

6 - charge, the errors in charge measurements include,

a. Al-foil charge/Faraday cup charge ± 1%

b. drift during run ± 4%

c. ionization chamber charge ± 2%

d. calibration of Faraday cup ± 3%

e. data analysis for random uncertainties ± 2%

Assuming that all these uncertainties are random, the overall uncertainty becomes ± 12%.

MICRODOSIMETRY

These microdosimetric data were obtained with a Rossi-type spherical proportional counter, 2.5 cm in diameter with a 0.3 cm thick wall, constructed from Shonka A150 tissue-equivalent plastic. The counter was embedded in a cylinder of A150 plastic 5.3 cm in diameter and 6 cm long. The tissue-equivalent proportional gas used was 55.0% C_3H_8, 39.6% CO_2, and 5.4% N_2 by volume. The filling pressure was 34 Torr, corresponding to a cell 2 micrometers in diameter. A LET detector 1.3 cm in diameter was positioned off-axis and used as a monitoring device.

The general methods used for the measurements and for data analysis have been described in detail elsewhere.[16,17]

Microdosimetric distributions for the eight cases are illustrated in Fig. 11 and some pertinent data are listed in Table IV. A comparison of several specific cases are shown in Fig. 12. In Fig. 11, the dose per unit logarithmic interval of lineal energy, yd(y), is plotted as a function of the logarithm of lineal eneryg, y, so that the area between two values of y is proportional to the fraction of the dose in the corresponding interval of y. The curves are normalized so that $\int_0^\infty d(y)\, dy = 1$. Qualitatively, there are four distinct regions of interest in each spectrum. First, there is a secondary electron distribution extending from about 10^{-2} keV/μm to about 10 keV/μm. The higher y portion of this distribution is obscured by the proton distribution extending from about 1 keV/μm to about 140 keV/μm. The distribution peaking at 250 keV/μm and extending to about 350 keV/μm is a result of alpha particles, and the events at higher lineal energies are from heavy ions. The fractions of the total dose which result from these various regions are listed in Table IV.

A comparison of spectra from 65 MeV protons incident on Li and Be shows that the major difference between the thick and thin targets is the lower gamma ray contribution in the neutron spectra from thick targets probably because of internal photon absorption and scattering in the target. The p-Be distributions show a higher contribution of high lineal energy (high stopping power) protons compared to the p-Li distributions. This result is

consistent with the larger component of low energy neutrons present in the incident neutron beam from Be as measured with the time-of-flight technique.

There are two major differences in the microdosimetric spectra for neutrons produced by protons at 65 MeV and at 35 MeV. For the neutrons created by protons of higher energy there is a definite shift to lower values for the minimum lineal energy observed for the corresponding recoil protons. There is also a corresponding decrease in the relative number of protons with higher lineal energy. It is interesting to note, however, that there are no significant changes in the contributions above 150 keV/μm which result from alpha particles and heavy ions. Therefore, the spectra at higher energies have a lower dose mean lineal energy.

At 35 MeV the deuteron produced neutron beams have approximately half the gamma ray component as compared to the proton produced ones. There is also a larger contribution of low energy recoil protons (high y) for the proton produced beams, which could be explained by the presence of a larger proportion of low energy neutrons. These lower energy neutrons tend to produce relatively less alpha particles and heavy ions so there is a corresponding decrease in the component of the dose from events above 150 keV/μm. This agrees qualitatively with what one would expect from the nuclear mechanisms involved.

Table IV

Particle	Incident Energy (MeV)	Target (cm)	Estimated Gamma Ray Component	$\int_{15}^{150} d(y)dy$	$\int_{150}^{\infty} d(y)dy$	$\bar{y}_D$ (keV/μm)
p	35	Li 3.84	0.07	0.42	0.11	69
p	35	Be 1.16	0.06	0.47	0.10	68
d	35	Li 3.84	0.03	0.38	0.13	75
d	35	Be 1.16	0.04	0.40	0.14	80
p	65	Li 5.33	0.04	0.30	0.12	68
p	65	Li 7.99	0.03	0.31	0.12	70
p	65	Be 1.60	0.05	0.33	0.11	66
p	65	Be 2.41	0.02	0.35	0.12	69

DISCUSSION

This experiment to characterize physically some neutron beams has rendered results in excellent agreement with available data. However, most of the results are new.

Energy Spectra

At 65 MeV, the thickest targets have a lower neutron yield

in the 10-20 MeV region than the thinner ones. This is interpreted as due to neutron scattering in the target. Hence, it is to be expected that the thicker targets must have a larger relative yield of low energy neutrons and a lower average neutron energy. The lithium targets produced more neutrons above 30 MeV per incident proton than the beryllium targets of equivalent thickness.

At 35 MeV, the p-Li and the p-Be neutron spectra have a larger proportion of high energy neutrons than the d-Li and d-Be neutron spectra. Again, lithium targets produce larger neutron fluxes toward the kinematic energy limit than beryllium targets. The neutron yield per incident charge particle is much greater for deuterons than for protons independent of target material. This is in agreement with stripping theory.[18]

Central Axis Depth Dose Distributions

The measured neutron dose distributions are in good qualitative agreement with the measured neutron energy spectra.

At 65 MeV, p-Li neutron beams produce more dose per incident proton and are more penetrating than p-Be neutron beams, for targets of equivalent thicknesses. For both the Be- and Li-targets, as the target's thickness decreases, the neutron beams produce dose distributions with longer attenuation lengths.

At 35 MeV, the proton generated neutron beams have similar dose attenuation lengths to deuteron generated neutron beams. Thick lithium targets create more penetrating neutron beams than thick beryllium targets regardless of incident particle type.

Dose Build-Up at Small Depths

The depths at which D_{max} occurs is greater for neutron beams created in lithium than in beryllium targets of equivalent thickness, for the same incident energy and particle type.

The initial rate at which dose builds up versus depth is greater in beryllium targets than in lithium targets. Also, at 35 MeV, the proton induced neutron beams have higher initial build-up rates than deuteron induced neutron beams. These results are consistent with those expected from the neutron spectral measurements.

Microdosimetry

There are significant changes in the microdosimetric spectra as a function of target material, target thickness, type of incident particle, and initial energy of the incident particle. The distribution of recoil protons shift toward lower lineal energies as the neutron energies increase. However, the presence of lower energy neutrons in the spectra, such as in the cases of 35 MeV protons on ^{7}Li and ^{9}Be, can cause larger numbers of high LET recoil protons which result in a significant number of events near the Bragg edge for protons. These effects tend to be compensated by the increase in heavy ion events at higher energies so that there is almost no change in the dose mean lineal energy for 65 MeV incident protons as compared to 35 MeV. The lack of change in the dose mean lineal energy, or correspondingly the dose mean LET, is somewhat surprising in that those changes in the neutron fluence spectra as measured by the time-of-flight technique do

result in corresponding changes in the microdosimetry spectra, at least qualitatively.

Rodgers et al.,[19] have measured microdosimetric spectra for 15 MeV neutrons from deuterons of thick tritium targets and Oliver et al.,[20] have obtained spectra for 16, 30 and 50 MeV deuterons on thick beryllium targets. The 15 MeV data show a higher contribution above 150 keV/μm (about 16%) than any of the present data with a corresponding higher dose mean lineal energy (about 90 keV/μm).

Oliver et al.,[20] obtained lower limits for the dose mean LET which correspond to dose mean lineal energies ($\bar{Y}_D = \frac{8}{9}\bar{L}_D$) of 57, 55 and 79 keV/μm at incident energies of 16, 30 and 50 MeV, respectively. These values are lower limits because data were obtained only in the interval of 1 to 500 keV/μm. The present results show significant data above 500 keV/μm, and the dose mean lineal energies are strongly influenced by the larger events. Therefore, it seems that the present results are consistent with those of Oliver et al.

Although there are observable differences in the measured microdosimetric distributions, it is still difficult to predict biological effects from these differences.

CONCLUSIONS

1. The energy spectra of neutron beams resulting from proton reactions may be affected differently as a function of depth in tissue than from deuteron induced neutron beams. This would be a consequence to the relatively larger fluxes of low energy neutrons in proton than in deuteron generated neutron beams.

These changes due to scattering ("filtration") may be significant in microdosimetry, as well as biological effects.

2. The aobve mentioned quantities, as well as depth dose distributions and the initial rate of dose build up versus depth may be affected by "filtration" (or "hardening") of the neutron beam with hydrogenous absorbers followed by recoil proton absorbers.

3. Lithium and beryllium targets of equivalent thicknesses when bombarded with protons create neutron beams of rather similar neutron characteristics.

4. The measured neutron dose rates are in good agreement with those reported by other workers. See Figure 13.

The choice between these two target materials will have to be made on the basis of dosimetric and technological considerations. From the point of view of accelerator technology, beryllium is a better target material because of low vapor pressure at high temperatures, high melting point, ease of machining, adequate heat conduction and chemical inertness.

Further Studies

Further studies should be carried out to study the effects of "filtering" of neutron beams on dose build up at small depths, energy spectras, depth-dose distributions, and microdosimetric properties of these and similar neutron beams in air and in-phantom as a function of depth.

REFERENCES

[1]H. Amols, et al. "Fast Neutron Dosimetry and Ion Linear Accelerators", LA-UR-76-1007 (1976).

[2]F. H. Attix, L. S. August, P. Shapiro and R. B. Theus, "The Physics and Dosimetry of Fast Neutrons for Radiotherapy", NRL Memorandum Report 3123, Sept. 1975.

C. J. Parnell, G. D. Oliver, P. R. Almond, J. B. Smathers,"The Dose Rate of Cyclotron Produced Fast Neutron Beams", Phys. Med. Biol. 17, 429 (1972).

L. S. August, R. B. Theus, F. H. Attix, R. O. Bondelid, P. Shapior, R. E. Surrat and C. C. Rogers, "Fast Neutron Dose Rate as a Function of Incident Deuteron Energy for D + Be", Phys. Med. Biol. 18, 641 (1973).

[3]J. A. Jungerman and F. P. Brady, "A Medium-Energy Neutron Facility", Nucl. Instr. Meth. 89, 167 (1970).

[4]J. F. Janni, "Calculations of Energy Loss, Range, Pathlength, Straggling ..... for 0.1 to 1000 MeV Protons", AFWL-TR 65-150 (Sept. 1966).

[5]M. W. McNaughton, N. S. P. King, F. P. Brady and J. L. Ullmann, "Improved Predictions of Neutron Detection Efficiency Resulting from new Measurements of $^{12}C(n,P)$ and $^{12}C(n,d)$ Reactions at 56 MeV", Nucl. Instr. Meth. 129, 241 (1975).

[6]P. Urone, private communication.

[7]S. W. Johnsen, "p-Be Neutron Production at 25 to 55 MeV", to appear in Med. Phys.

[8]J. A. Jungerman, F. P. Brady, W. J. Knox, T. Montgomery, M. R. McGie, J. L. Romero and Y. Ishizaki, "Production of Medium-Energy Neutrons from Proton Bombardment of Light Elements", Nucl. Instr. Meth. 94, 421 (1971).

[9] J. P. Meulders, P. Leleux, P. C. Maig and C. Pirat, "Fast Neutron Yields and Spectra from Targets of Varying Atomic Number Bombarded With Deuterons from 16 6o 50 MeV", Phys. Med. Biol. 20, 235 (1975).

[10] F. H. Attix, R. B. Theus, S. G. Gorbics and C. C. Rogers, "Report on NRL Measurements as a Participant in the INDI", NRL Memorandum Report 3051, May 1975.

J. J. Broerse, C. J. Bouts, F. A. Van Galsteren, A. C. Engels, J. S. Groen, B. Hogeweg, H. B. Kal, L. A. Reeder, H. A. Versteegh, F. A. C. Wijnants and J. Zoetelief, "Experimental Arrangement for European Neutron Dosimetry Intercomparison Project (ENDIP) Performed at TNO", Workshop on Basic Physical Data for Neutron Dosimetry, Rijswijk, The Netherlands, May 19-21, 1976.

[11] J. B. Smathers, V. A. Otte, A. R. Smith, P. R. Almond, F. H. Attix, J. J. Spokas, W. M. Quam and L. J. Goodman, "Composition of A-150 Tissue Equivalent Plastic", submitted for publication to Med. Phys.

[12] EG&G, Inc., Goleta, California 93017, model IC-18.

[13] A. R. Smith, P. R. Almond, J. B. Smathers, V. A. Otte, F. H. Attix, R. B. Theus, P. Wootton, H. Bichsel, J. Eemaa, D. Williams, D. K. Bewley and C. J. Parnell, "Dosimetry Intercomparisons Between Fast Neutron Radiotherapy Facilities", Med. Phys. 2, 195 (1975).

[14] N. A. Frigerio, R. F. Coley and M. J. Sampson, "Depth Dose Determinations, I. Tissue Equivalent Liquids for Standard Man and Muscle", Phys. Med. Biol. 17, 792 (1972).

[15] EG&G, Inc., model EIC.

[16] J. F. Dicello, W. Gross and U. Kraljevic, "Radiation Quality of Californium-252", Radiat. Res. 17, 345-355 (1972).

[17]H. I. Amols, J. F. Dicello and T. F. Lane, "Microdosimetry of Negative Pions". Proceedings of the Fifth Symposium on Microdosimetry, Verbanica, Pallanza, Italy. EURATOM ERU5452d-e-f (9/22-26/76).

[18]L. S. August, F. H. Attix, P. Shapiro, R. B. Theus, G. Herling, and C. C. Rogers, "Stripping-Theory Analysis of Thick-Target Neutron Production for D + Be", in press, Phys. Med. Biol.

[19]R. Rodgers, J. F. Dicello and W. Gross, "Event Distributions from Monoenergetic Neutrons", Radiobiological Research Labaratory, Columbia University, New York. Annual Report COO-3243-1, 52-59 (1972).

[20]G. D. Oliver, Jr., W. H. Grant and J. B. Smathers, "Radiation Quality of Fields Produced by 16-, 30- and 50-MeV Deuterons on Beryllium", Radiant Res. 61, 366-373 (1975).

[21]P. Heintz, G. Hendry, S. W. Johnsen, W. Quam, R. B. Theus and J. Tom, private communication.

FIGURE CAPTIONS

Fig. 1 Spectra of neutrons produced by bombarding beryllium targets with 65.4 MeV protons. The target thickness used to produce each spectrum are: curve A, 2.41 cm; curve B, 2.21 cm; curve C, 1.96 cm; curve D, 1.60 cm. The ordinate is in units of 10^9 n sr^{-1} μC^{-1}.

Fig. 2 Spectra of neutrons produced by bombarding lithium targets with 65.4 MeV protons. The target thickness used to produce each spectrum is) curve A, 7.99 cm; curve B, 7.34 cm; curve C, 6.50 cm; curve D, 5.33 cm. The ordinate is in units of 10^9 n sr^{-1} μC^{-1}.

Fig. 3 Spectra of neutrons produced by stopping 35 MeV protons and deuterons in lithium and beryllium. Curves A and B: 35 MeV protons stopping in beryllium and lithium respectively; full scale = 1.5 x 10^9 neutrons/microCoulomb/steradian/MeV. Curves C and D: 35 MeV deuterons stopping in beryllium and lithium respectively; full scale = 1.5 x 10^{10} neutrons/microCoulomb/steradian/MeV.

Fig. 4 Central axis depth dose measurements in a water phantom, at 351 cm TSD 65 MeV protons are incident on lithium targets of various thicknesses.

Fig. 5 Central axis depth dose measurements in a water phantom at 351 cm TSD 65 MeV protons are incident on beryllium targets of various thicknesses.

Fig. 6 Central axis depth dose measurements in a water phantom, at 351 cm TSD 35 MeV protons are incident on beryllium and lithium thick targets.

Fig. 7 Central axis depth dose measurements in a water phantom at 351 cm TSD 35 MeV deuterons on thick lithium and beryllium targets.

Fig. 8 Dose build-up in tissue equivalent plastic. 65 MeV protons incident on beryllium targets. The special symbol shows Fermilab results.

Fig. 9 Dose build-up in tissue equivalent plastic. 65 MeV protons incident on lithium targets.

Fig. 10 Dose build-up in tissue equivalent plastic. 35 MeV protons and 35 MeV deuterons are incident on lithium and beryllium targets.

Fig. 11 Differential and integral doses as a function of lineal energy for protons and deuterons incident on thick and thin Be- and Li-targets.

Fig. 12 Differential dose per unit logarithm of the lineal energy versus lineal energy for neutrons due to protons and deuterons incident on beryllium and lithium targets. The figures in parenthesis show incident particle energy. In all cases the targets are longer than the incident particle ranges.

Fig. 13 Dose rate for neutrons produced by protons or deuterons incident on Be- or Li-targets. The solid triangles (▲) and circles (●) are the present results. The solid

squares (■) are unpublished data obtained by Heintz et al.[21] The open squares (□) are data from Attix et al.[2] The remaining points are from a review of d-Be data by Parnell et al.[2]

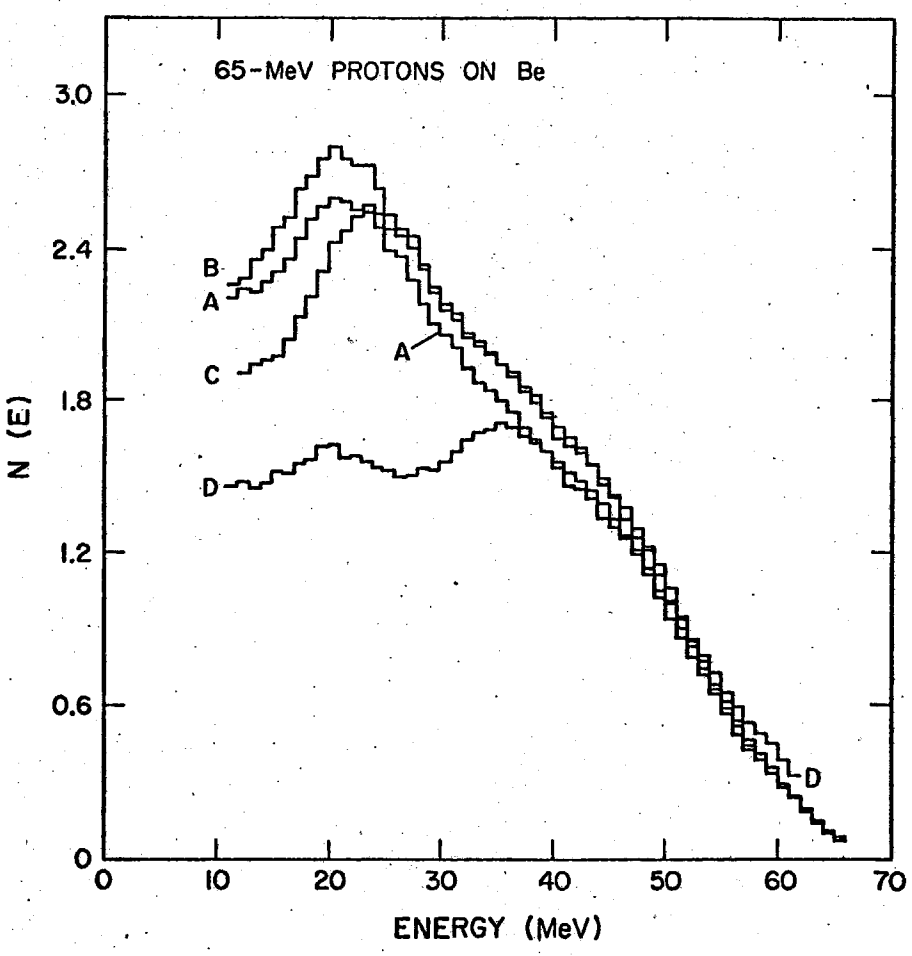
65-MeV PROTONS ON Be
3.0
2.4
1.8
1.2
0.6
0
N (E)
B
A
C
A
D
D
0
10
20
30
40
50
60
70
ENERGY (MeV)

Fig. 1

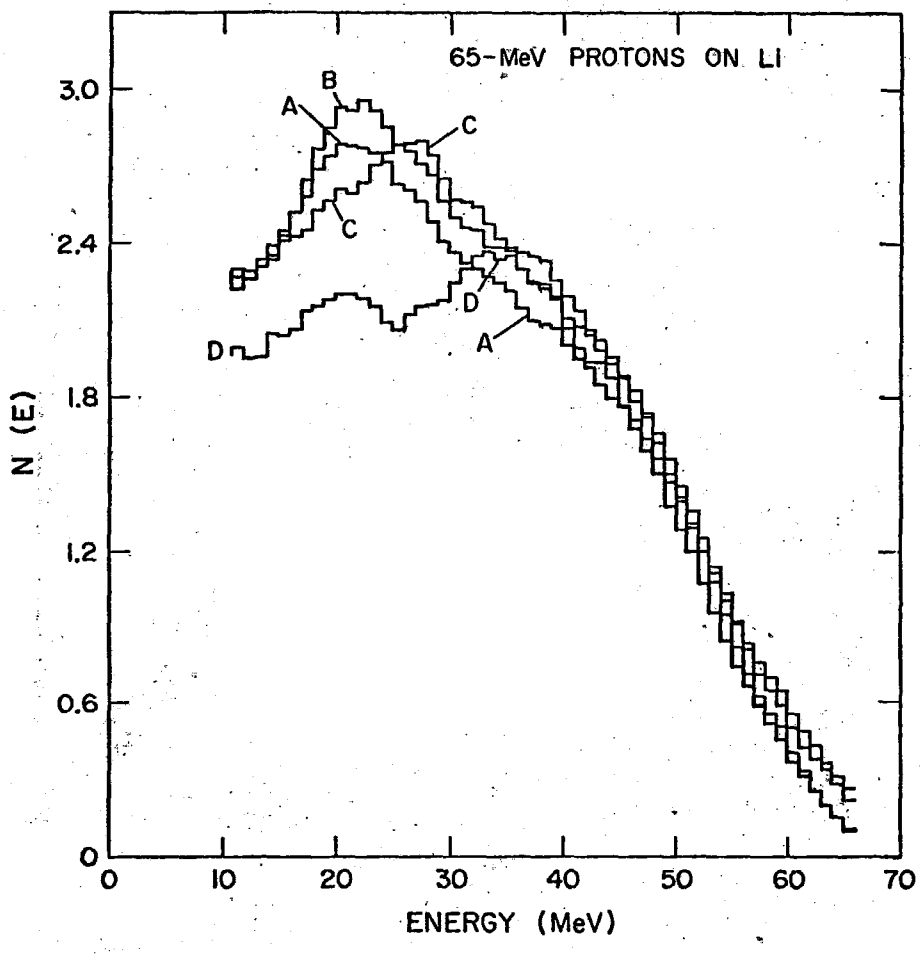
65-MeV PROTONS ON LI
N (E)
ENERGY (MeV)
A
B
C
D

Fig. 2

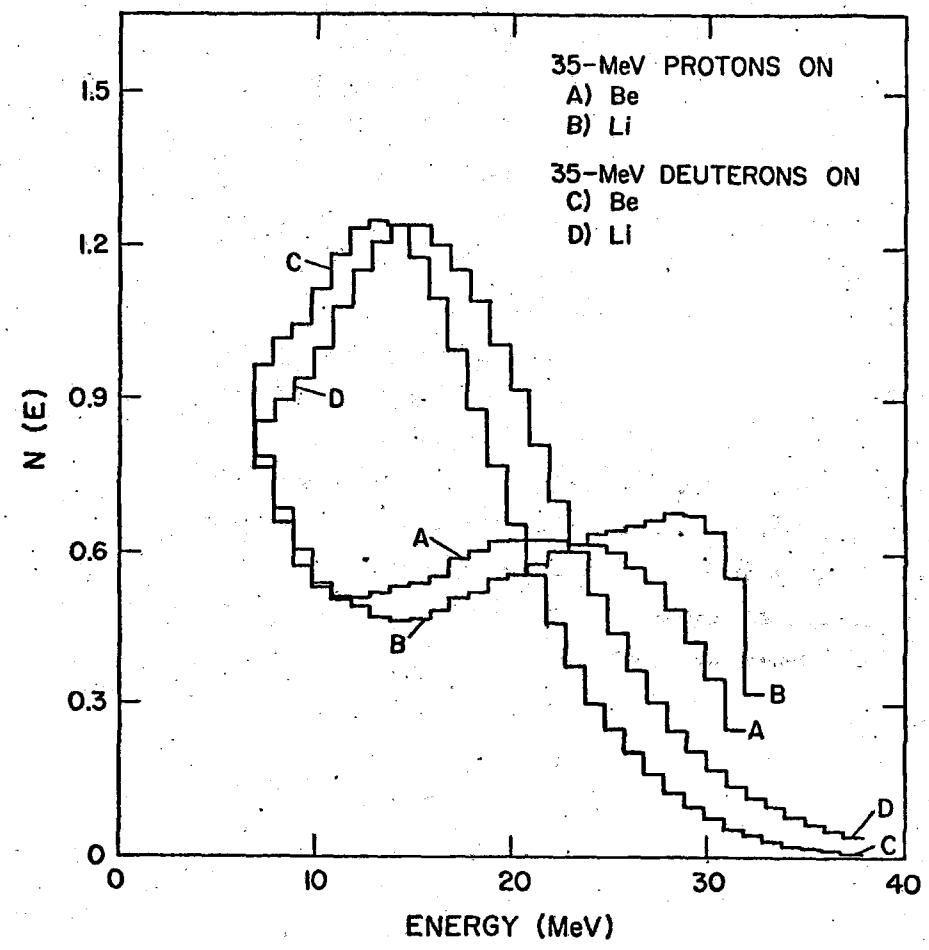
35-MeV PROTONS ON
A) Be
B) Li
35-MeV DEUTERONS ON
C) Be
D) Li
N (E)
ENERGY (MeV)

Fig. 3

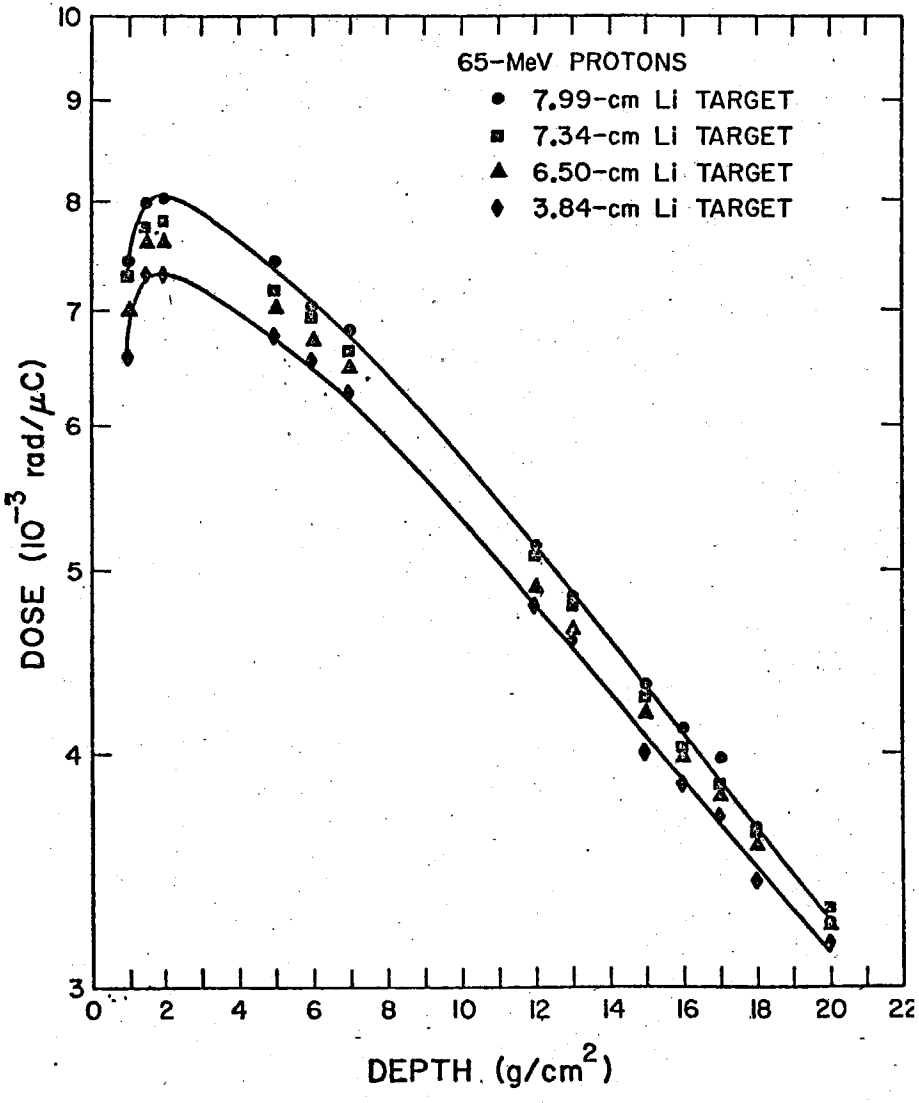
65-MeV PROTONS
7.99-cm Li TARGET
7.34-cm Li TARGET
6.50-cm Li TARGET
3.84-cm Li TARGET
DOSE (10^{-3} rad/μC)
DEPTH (g/cm^2)

Fig. 4

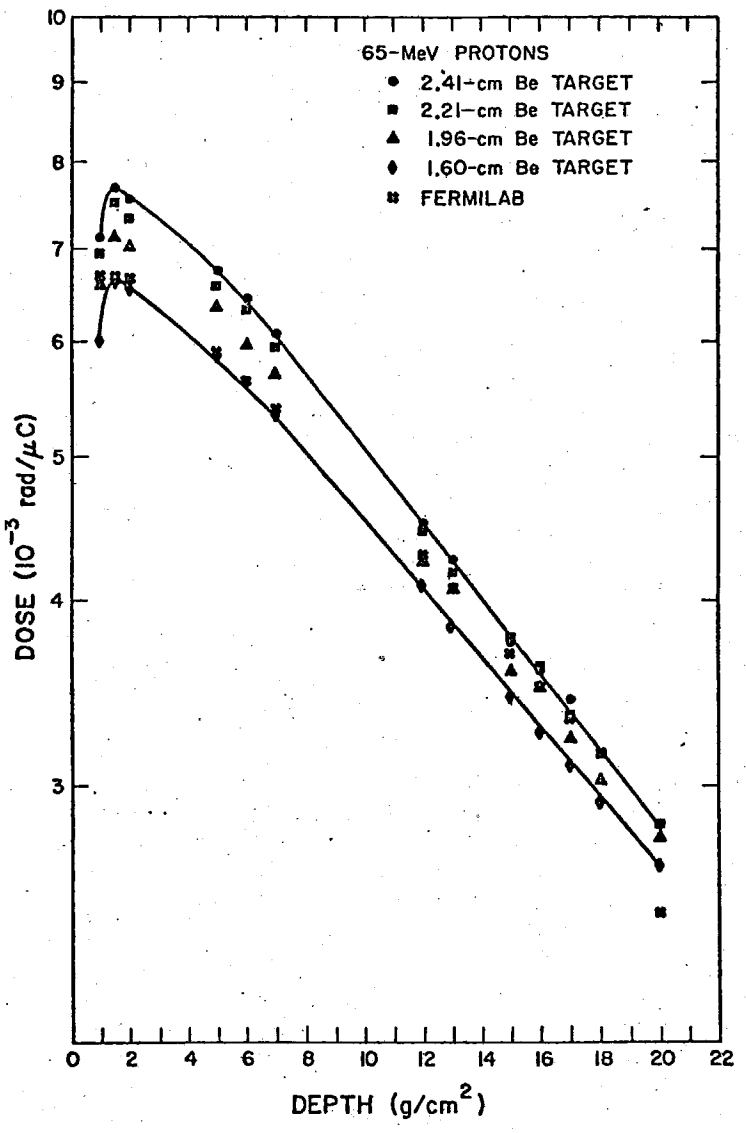
65-MeV PROTONS
2.41-cm Be TARGET
2.21-cm Be TARGET
1.96-cm Be TARGET
1.60-cm Be TARGET
FERMILAB
DOSE (10^{-3} rad/μC)
DEPTH (g/cm^2)

Fig. 5

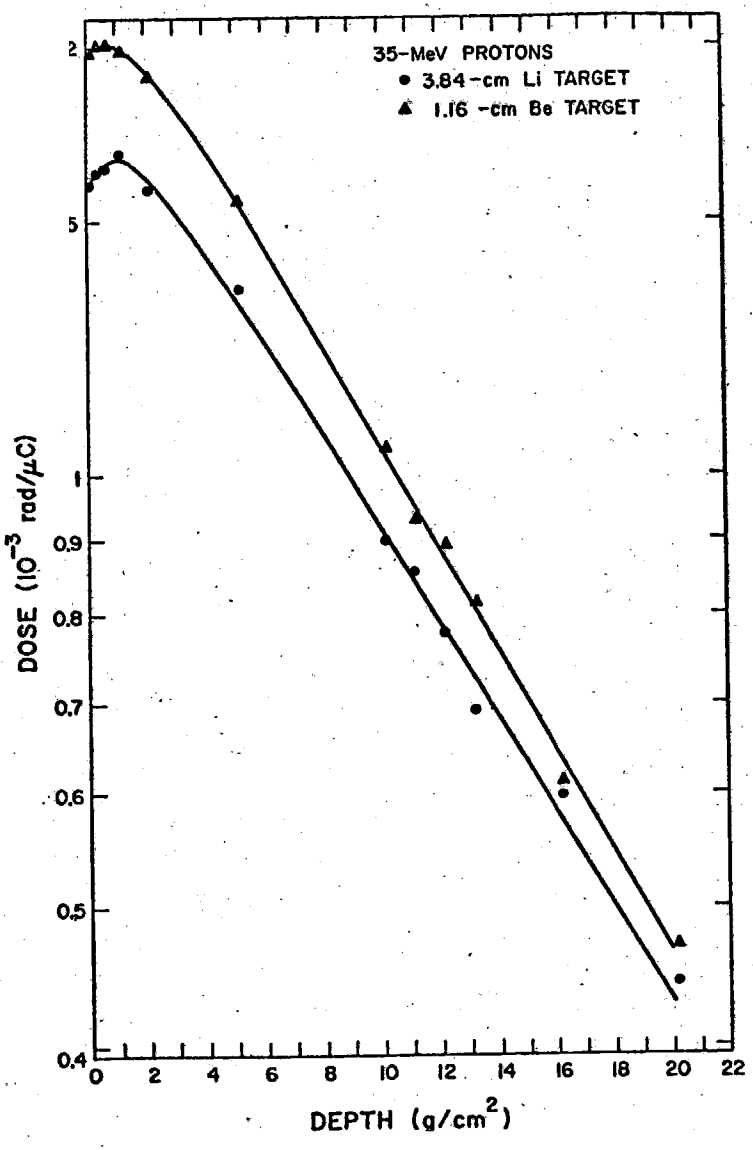
35-MeV PROTONS
● 3.84-cm Li TARGET
▲ 1.16-cm Be TARGET
DOSE (10^{-3} rad/μC)
DEPTH (g/cm^2)

Fig. 6

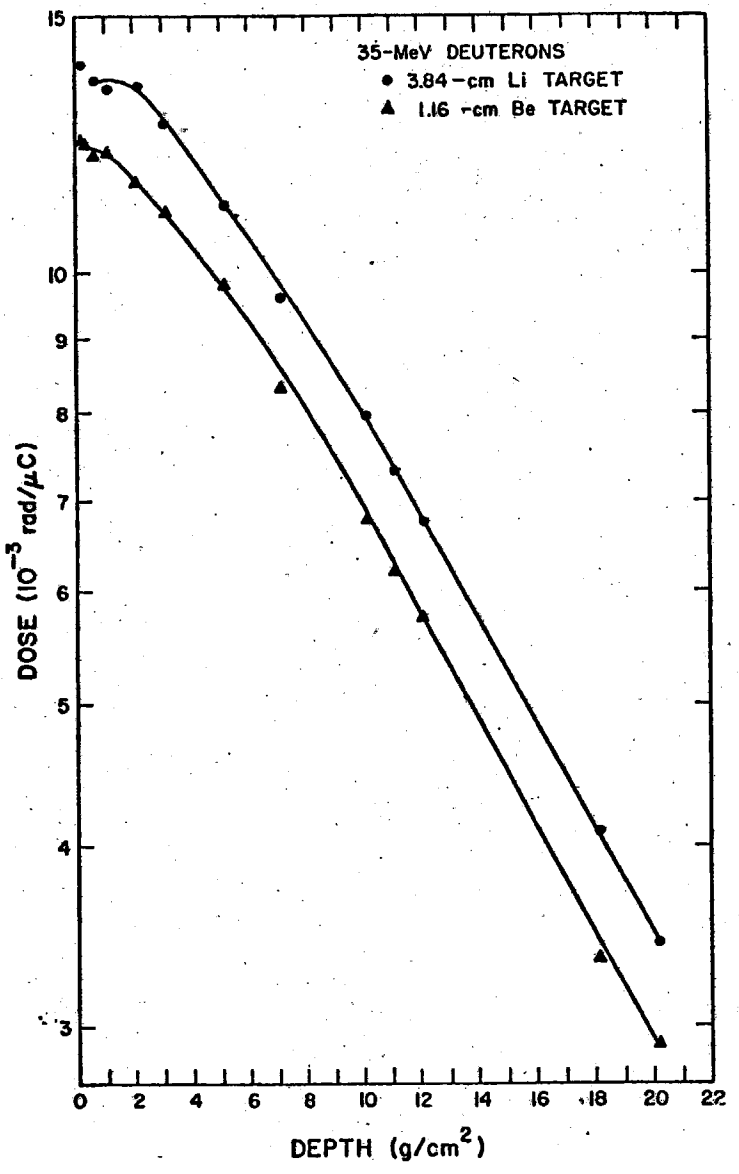
35-MeV DEUTERONS
● 3.84-cm Li TARGET
▲ 1.16-cm Be TARGET
DOSE (10^{-3} rad/μC)
DEPTH (g/cm^2)

Fig. 7

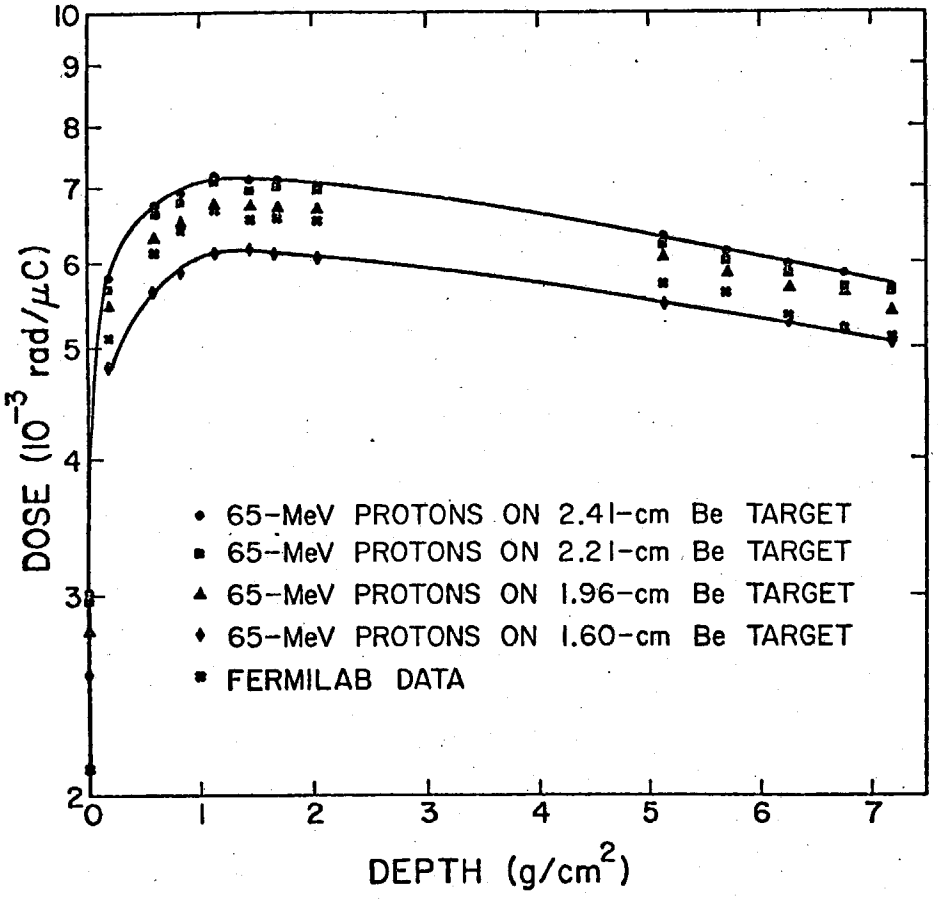
DOSE (10^{-3} rad/μC)
DEPTH (g/cm^2)
• 65-MeV PROTONS ON 2.41-cm Be TARGET
▪ 65-MeV PROTONS ON 2.21-cm Be TARGET
▲ 65-MeV PROTONS ON 1.96-cm Be TARGET
♦ 65-MeV PROTONS ON 1.60-cm Be TARGET
* FERMILAB DATA

Fig. 8

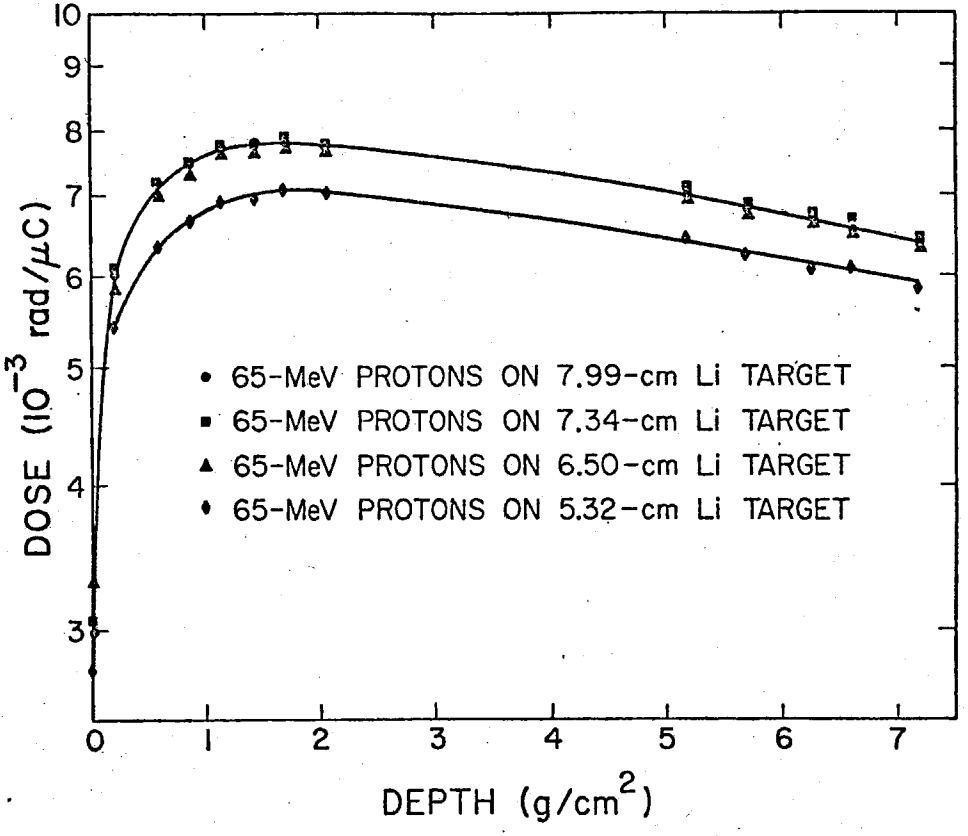
DOSE (10^{-3} rad/μC)
DEPTH (g/cm^2)
• 65-MeV PROTONS ON 7.99-cm Li TARGET
▪ 65-MeV PROTONS ON 7.34-cm Li TARGET
▲ 65-MeV PROTONS ON 6.50-cm Li TARGET
♦ 65-MeV PROTONS ON 5.32-cm Li TARGET

Fig. 9

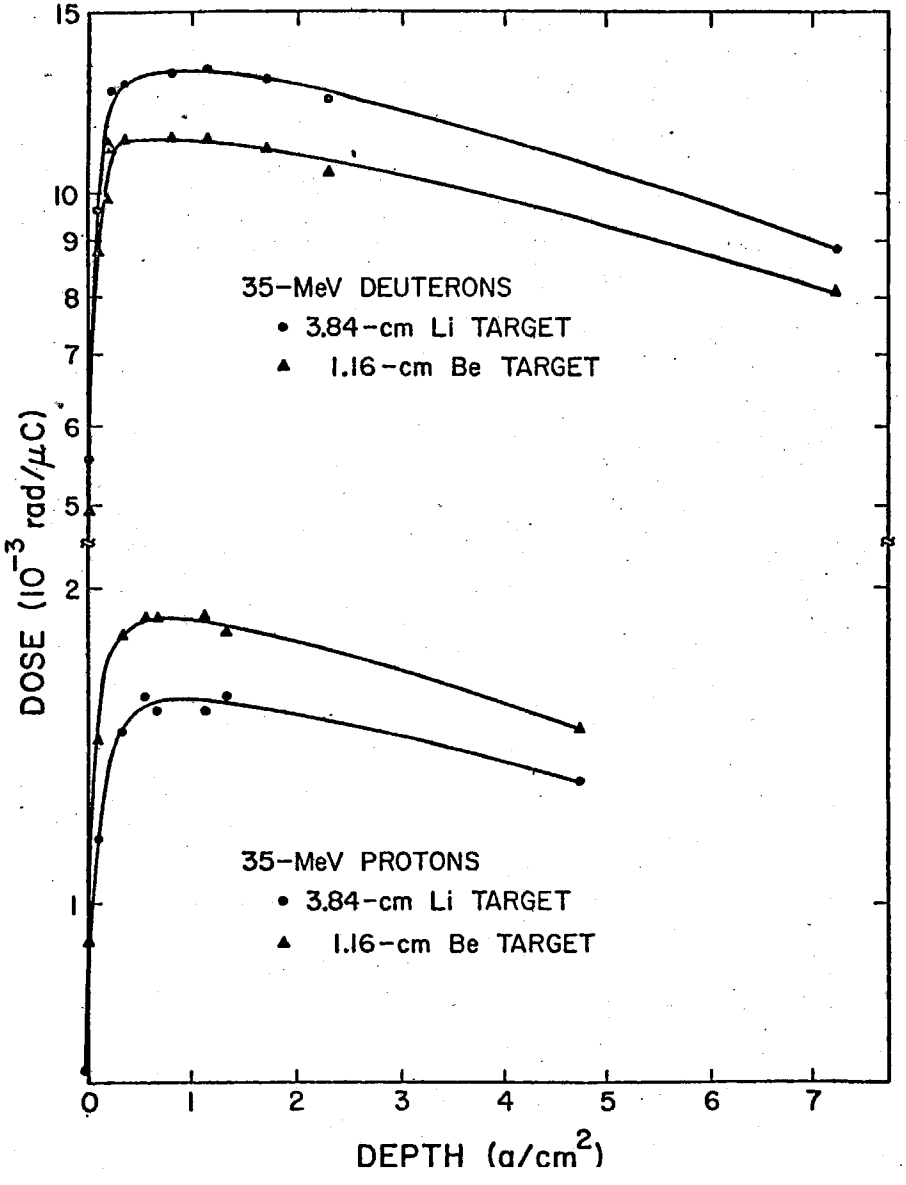
35-MeV DEUTERONS
• 3.84-cm Li TARGET
▲ 1.16-cm Be TARGET
35-MeV PROTONS
• 3.84-cm Li TARGET
▲ 1.16-cm Be TARGET
DOSE (10^{-3} rad/μC)
DEPTH (g/cm^2)

Fig. 10

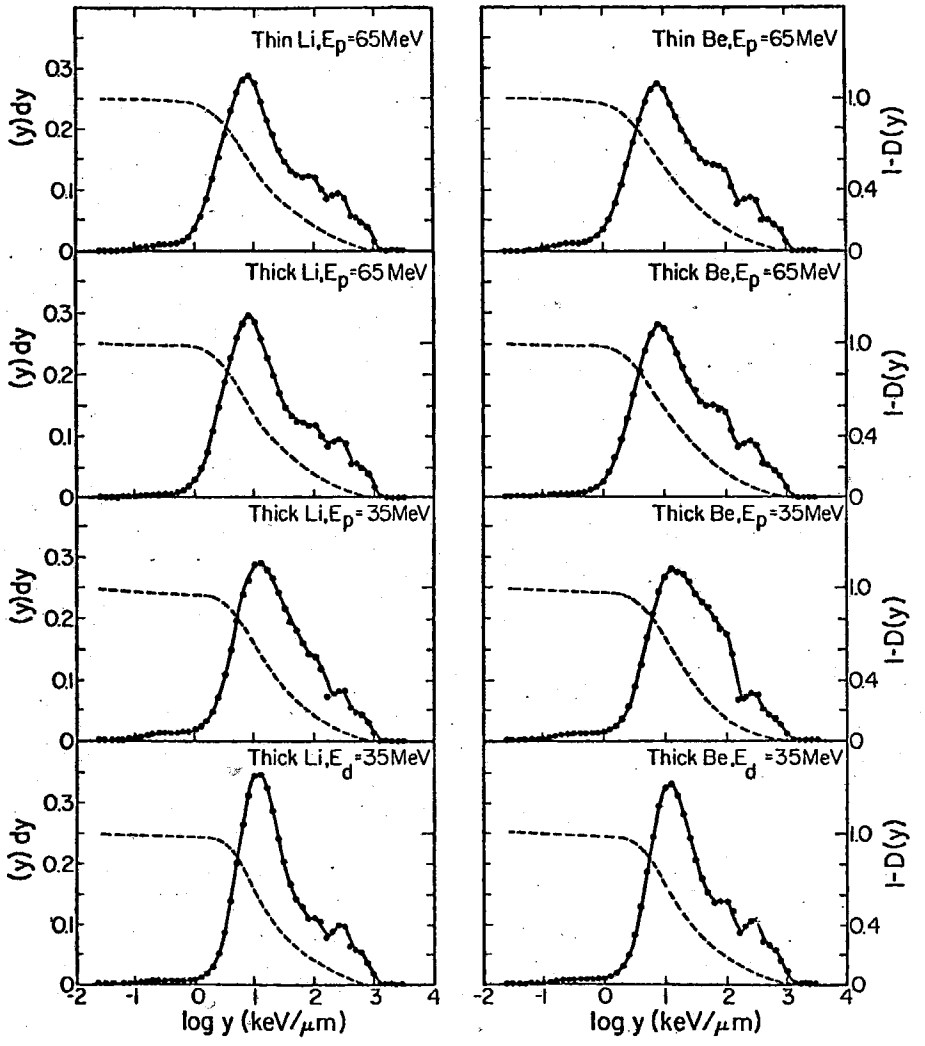
Thin Li,Ep=65MeV
Thin Be,Ep=65MeV
Thick Li,Ep=65MeV
Thick Be,Ep=65MeV
Thick Li,Ep=35MeV
Thick Be,Ep=35MeV
Thick Li,Ed=35MeV
Thick Be,Ed=35MeV
(y)dy
I-D(y)
log y (keV/μm)

Fig. 11

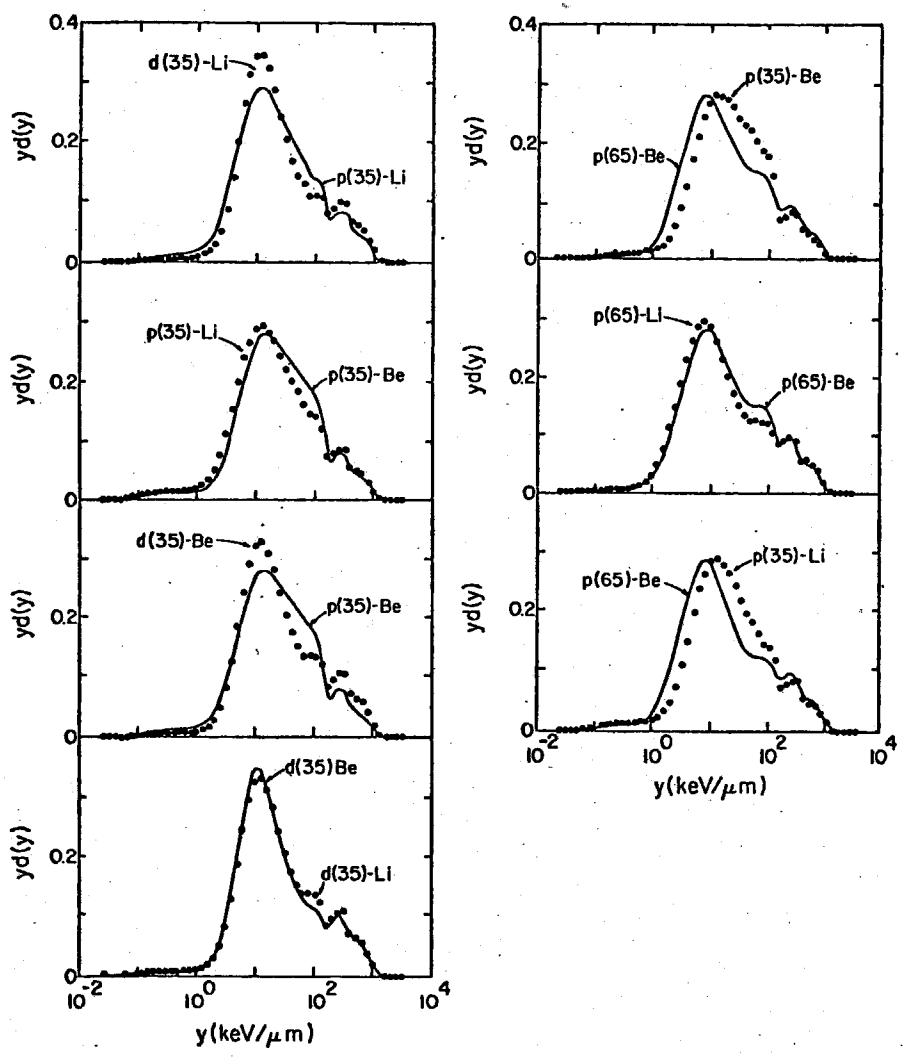
d(35)-Li
p(35)-Li
p(35)-Be
d(35)-Be
d(35)Be
d(35)-Li
p(65)-Be
p(65)-Li
yd(y)
y(keV/μm)

Fig. 12

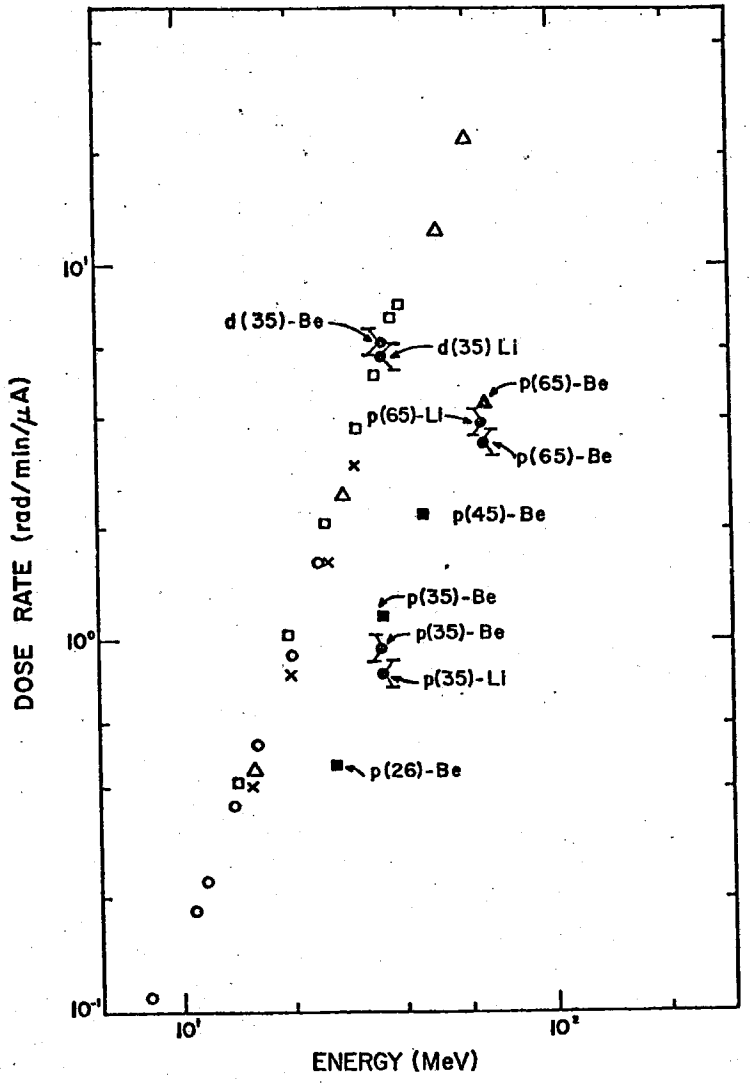
d(35)-Be
d(35) Li
p(65)-Be
p(65)-Li
p(65)-Be
p(45)-Be
p(35)-Be
p(35)-Be
p(35)-Li
p(26)-Be
DOSE RATE (rad/min/μA)
ENERGY (MeV)

Fig. 13